International Journal Of Scientific & Engineering Research, Volume 7, Issue 6, June-2016
ISSN 2229-5518

Aerodynamic Internal Pressure Loads Applied On Nonstructural Elements under Wind Gusts

Sreenadh Chevula*, Ángel Sanz-Andres, Sebastián Franchini.
Instituto Universitario de Microgravedad 'Ignacio da Riva', Universidad Politécnica de Madrid (IDR/UPM),
ETSI Aeronáuticos, Plaza del Cardenal Cisneros, 3, E-28040, Madrid, Spain.
* Corresponding author, Tel.: +34 91 3366353, Fax: +34 91 3366363, E-mail: Sreenadh.Chevula@upm.es

Abstract—Vent holes can be used to reduce the aerodynamic pressure loads on nonstructural elements of buildings. The analysis of these loads applied on nonstructural elements of buildings (window panes, closure panels, etc.) with vent holes, under gusty wind conditions, have been studied both experimentally and employing a theoretical model. An experimental setup based on an open circuit, closed test section, and low speed wind tunnel, designed and built at the Instituto de Microgravedad "Ignacio Da Riva" of the Universidad Politécnica de Madrid (IDR/UPM) has been used. A mechanism in the wind tunnel generates sinusoidal gusty winds inside the test section. Theoretical predictions of the pressure loads have been obtained using a mathematical model based on the mass conservation equation and polytropic law gas evolution. In the experimental setup, an air reservoir with a vent hole has been selected as a model to simulate the internal pressure loads acting on the walls of a building under a tangential unsteady (gusty) flow. The pressure jumps developed across the vent holes have been studied as a function of vent hole size, air reservoir volume, and gust frequency. In this work, the results for the case of small pressure jumps across the vent hole have been presented, which is the case of most practical interest, in order to reduce the pressure load on the elements.
The evolution of the pressure loss coefficient ξ, at unsteady flow conditions has been studied, and it has been found that its value is not constant in a gusty wind, but depends both on the frequency of the gust and on the direction of the flow through the vent hole (either inhalation or exhalation).

Index Terms— Aerodynamic internal pressure loads, Vent holes, Gusty winds, Ventilation, Non-linear model

1. Introduction

When wind flows over a building, it produces a spatially and temporally varying external pressure distribution on the external surface of the building. The pressure inside the building depends on wind characteristics and on external surface pressure, the position and size of all openings connecting the exterior to the interior of the building, and the effective volume of the building. Internal pressure fluctuations in a nominally sealed building are generally small in magnitude compared to external pressures. On the one hand the failure of a door or window on the building can create a dominant opening and generate large internal pressures in strong winds that contribute a significant proportion to the total (i.e., net) design wind loads. On the other hand the internal pressures in combination with large external pressures acting in the same direction are a common cause of roof and wall failures in windstorms and are often the governing design criterion for both the cladding and structural components of a building. The study of the internal pressure loads induced by gusty winds on buildings has traditionally received less attention than external pressure studies [1]. Concerning the internal pressure study at steady flow conditions, Euteneuer [2] was probably the first to study these internal pressures within a building with a large opening in a wall. He derived an expression for the response time of the pressure in a building subjected to a sudden change in external pressure such as that caused by a sudden failure of a window, neglecting inertial effects on the flow through the opening. But when a sudden opening is created, the transient response of internal pressure may present the damped oscillations which produce an initial overshoot significantly higher than the mean external pressure at the opening [1, 3]. Therefore, an un-estimated opening in buildings under high wind events such as tropical cyclones can create a failure of overloaded building components (due to the impact of flying debris) [4]. The interaction between the internal pressure fluctuations and the building envelope under both steady and unsteady flows can be complex and is further complicated by the often meagre knowledge of key parameters such as the vent position, the size and the flow through the vent hole [5]. The accuracy in the values of the above mentioned parameters can help to avoid the failures and unwanted ventilations of the buildings. For the formulation of the internal pressure loads under steady and unsteady conditions, various research works can be found from the scientific world such as Liu and Rhee [6] who further examined the phenomenon of Helmholtz resonance in a building model for the cases of an opening on a windward and a leeward wall, and with both low (1%) and moderate (10%) turbulence intensities in the approach flow. They also studied the excitation of the resonance by the vortex shedding from a circular cylinder upwind of the opening. Vickery et al. [7] studied the dynamics of internal pressures in buildings with a large opening at model scale, and proposed a simplified relationship between the fluctuating internal and external pressures. They also carried out experiments on a model using a camera shutter as the opening. The internal volume of the model was connected to a larger volume beneath the wind tunnel to satisfy the scaling requirements for internal pressure fluctuations, as discussed by Holmes [1]. Using this equipment they studied the sudden opening case, as well as the response of the internal pressure to upwind turbulence. However, the turbulence intensity in the approach flow was lower than that expected in over-land winds in developed boundary layers in an atmospheric flow. Ginger et al. [8] carried out full scale-studies on internal pressure and showed that the mean and fluctuating internal pressure coefficients in a nominally

International Journal Of Scientific & Engineering Research, Volume 7, Issue 6, June-2016
ISSN 2229-5518

sealed building are smaller in magnitude than the pressure on the external surfaces and also reported that the mean and fluctuating internal pressure coefficients increase with increasing windward/leeward open area ratio. Sharma et al [9] studied Helmholtz resonance in a model of the Texas Tech Building for a full range of wind directions in simulated atmospheric boundary layer flow (about 20% turbulence intensity at roof height) and found the highest internal pressure fluctuations at a critical Strouhal Number when the opening was on a side wall for an oblique wind direction. However, their modelling did not include internal volume distortion as required to satisfy the correct non-dimensional scaling parameters described in Holmes [1, 10].

Kopp et al. [11] measured internal pressures in a model of a typical two-storey house located in open-country exposure with various combinations of windows and door openings. The model was compartmentalized into connected attic and living volumes, and with a backyard roof. From the measurements of the internal and external pressures (with a variety of combinations of the wall open areas) they concluded that Helmholtz resonance effects were small in these tests. Sharma et al. [12] predicted the building internal pressure gain functions by using computational and analytical modelling techniques. Sharma [13] studied the influence of the flexibility of the building envelope in the case of a low-rise building design with a dominant opening. He developed an analytical model for the problem of quasi-static loads acting on the envelope under gusty winds. This research showed that building envelope flexibility lowers the Helmholtz resonance frequency and increased damping in the internal pressure system (as indicated by the lowering of the resonant peak in the internal pressure admittance function).

Harris [14] developed a linearized theory of internal pressure for a nominally sealed building with lumped leakages in both windward and leeward orientation, which proved that the mean internal pressure is also influenced by external pressure fluctuations at the openings. A classical approach focused on the calculation of internal pressure relevant to the various building models can be found in Holmes [15].

Chaplin [16] obtained experimental data and analyzed them with the help of a linearized mathematical model. Chaplin et al [17] analyzed the mechanism of building ventilation by using a non-linear oscillator model as a function of two parameters (internal pressure of the building and pressure loss coefficient). They compared the obtained results with the results presented in Chaplin [16] and concluded that the theoretical and experimental gain factors, obtained with standard values of the pressure loss coefficients, were in good agreement. However, experimentally determined values of the inertial coefficient [18] suggest that, for small opening diameters, the fundamental equation used in the theoretical derivation is not adequate, and that extra terms to describe centripetal accelerations should have been included [17]. In this paper, the non-linear methodology presented by Chaplin et al. [17] has been followed in some extent to analyze the evolution of the internal pressure.

Concerning the problem of the study of internal pressure, some additional interesting works can be found in the field of space technology such as space vehicle compartment vent (NASA SP-8060) [19]. The pressure variation inside a spacecraft (as a payload of a launch vehicle) during the climb through the atmosphere was analysed by Sanz-Andres et al. [20]. Ronald, et al. [21] proposed an analytical expression that can be used to estimate the size of the depressurization vents of equipment on board space launch vehicles and other applications.

From the above research works it can be observed that many investigators have applied linear models for the formulation of internal pressure loads in both steady and unsteady flow conditions. But, as will be explained in the following, an unsteady flow condition leads to an intrinsically nonlinear formulation and solution. Therefore, in this work a nonlinear model for analysing the internal pressure loads has been developed based on the following assumptions:

(a) The instantaneous pressure is uniform across the opening and inside the reservoir (internal volume) but changes with time.

(b) It is possible to adequately specify the pressure loss coefficient.

This paper is organized into the following sections: 2) the experimental setup and the integration of the testing model are presented; 3) based on the mass conservation equation and gas evolution polytropic law, a non-linear theoretical model is proposed; 4) the results of the experiments performed and the dependence of the pressure loss coefficients on the parameters that characterize unsteady flow conditions have been summarized; 5) conclusions.

2. Experimental setup

In this section the experimental setup to study the internal pressure changes in an air reservoir produced by outside pressure changes under several geometrical conditions has been presented. In the present work, the simulations of gusty winds under laboratory conditions is one of the major tasks. To obtain these gusty wind simulations, a sinusoidal gust generating mechanism wind tunnel, which was designed and built at the Instituto de Microgravedad "Ignacio Da Riva" of the Universidad Politécnica de Madrid (IDR/UPM), has been used. The theoretical model and research that justifies the development of this gust wind tunnel can be found in Sanz-Andres et al. [22]. The physical description and functioning of the gust wind tunnel are presented in Chevula [23, 25]. To achieve the aim of the present work a design has been proposed for the experimental setup which includes the following hardware components (see fig. 1 and 2):

- Air reservoirs with volumes V_R = 0.022 m^3, 0.011 m^3, 0.0062 m^3, 0.0033 m^3, and 0.0016 m^3 (relevant uncertainty = ± 0.00035 m^3).
- Vent hole radius , R_{vh} = 0.5 mm, 1.5 mm, 2.5 mm, 5 mm, 7 mm, 9 mm, 10 mm, 11 mm, and 12.5 mm (uncertainty = ± 0.8%).
- Pressure taps Pt_1, Pt_2 and Pt_3 to measure the internal and external pressures, P_0, P_e.
- A hot wire anemometer with 1D probe (to measure the reference flow speed in the test section, U^E).
- Two differential pressure transducers TR_1 (Sensor Technics, Model BTEL 5905 DIA; uncertainty = ± 0.5, time response (raise time) ≤ 2 m.s) and TR_2 (Honeywell, Model 1639CO1D75, uncertainty = ± 1.2 Pa, time response (raise time) ≤ 1.8 m.s) which measure the pressure differences $P_0 - P_e$ and $P_e - P_r$ respectively.

International Journal Of Scientific & Engineering Research, Volume 7, Issue 6, June-2016
ISSN 2229-5518

- Four connecting tubes of 70 cm length and 0.5 cm diameter.
- An auxiliar rigid air reservoir, which supplies the atmospheric pressure, P_r, as reference for pressure transducer TR_2.

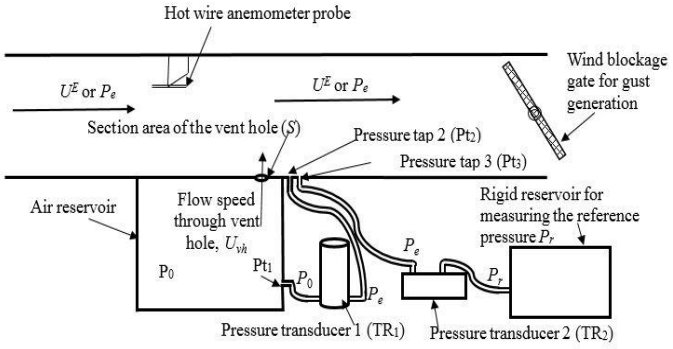

Figure 1. Schematic diagram of the experimental setup.

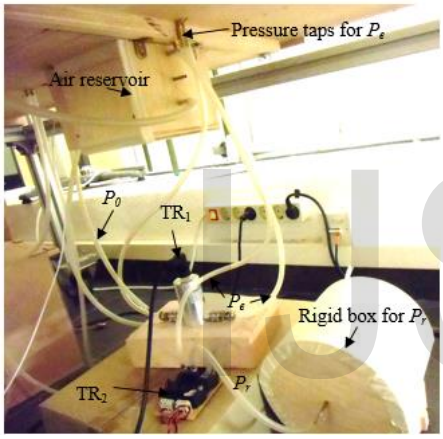

Figure 2. Experimental setup; same as fig.1.

2.1 *Integration of the experimental setup*

The configuration to be studied corresponds to the following problem. A building is placed in a gusty flow (unsteady fluid flow) condition. The interaction between the gusty wind and the building generates a pressure field outside the building associated to a tangential flow around the building. The pressure inside the building is uniform if the building has no leaks. However, in this situation large pressure differences between the internal and external pressure can appear. One method to reduce this pressure difference (or pressure jump) is to provide the rooms of the building with venting holes.

In order to simulate this configuration in laboratory conditions, the tangential unsteady flow outside the building is modelized as the flow inside the test section of a gust wind tunnel, and the room as a reservoir with a venting hole. In this experimental setup (fig.1), an air reservoir is fixed below the test section floor. Both the test section floor and air reservoir surface are connected with a vent hole. As a result, a gusty airflow can enter into the air reservoir. A 1D hot wire anemometer probe is attached to the ceiling of the test section to measure the reference flow speed U^E in the test section. Pressure taps Pt_1 and Pt_2 are connected to pressure transducer TR_1 to measure the pressure jump across the vent hole ΔP. Pressure tap Pt_3 and the reference atmosphere pressure (obtained from a rigid air reservoir) P_r are connected to pressure transducer TR_2 to measure the pressure increment inside the wind tunnel, ΔP_e (see fig. 1). A thorough check has been carried out to ensure no air leakage from the reservoir.

2.2 *Characterization of the flow measured in the test section*

In this paragraph, the characteristics of the flow measured in the test section by a hot wire anemometer, compared to sinusoidal time variations, are presented. The flow measurements are performed at nominal gust frequencies f_g^N = 2.4, 4.0, 6.0, and 7.7 Hz; mean speed of gusty winds U_{mv} = 2.5 to 5.5 m/s; gusts produced by rotating gates with blockage length L_{gc} = 380 mm, and the flow entering in the test section is smoothed by using a honeycomb plus a foam block at the entrance of the test section. More information about these parameters can be found in Chevula [23, 25]. From the experimental data it has been noted that the flow velocity measured by the hot wire anemometer probe follows a sinusoidal shape with some small drifts. By using a Matlab program the experimental data have been fitted to the sinusoidal function, U^F, given by

$$U^F = U^E_{mv} + U^E_a \sin(\omega t + \varphi), \qquad (1)$$

where U^E_a is the amplitude of the signal, U^E_{mv} is the mean value of measured flow, ω is the angular frequency, and φ is the phase referenced to wind blockage gate closing position (see fig. 1). Obtained values for these parameters are presented in table 1.

Table 1. Values of the fitted data of: flow speed U^E; amplitude, U^E_a; angular frequency, ω; phase, φ; and regression coefficient, R^2; from experimental data with fan motor speed f_m = 20, 30, and 40 Hz; nominal gust frequency f_g^N = 2.4, 4.0, 6.0, and 7.7 Hz; and rotating gate chord L_{gc} = 380 mm.

f_m [Hz]	20 (U^E_{mv} = 2.5 to 3.5 m/s)				30 (U^E_{mv} = 3.5 to 4.5 m/s)				40 (U^E_{mv} = 4.5 to 5.5 m/s)			
f_g^N [Hz]	2.4	4.0	6.0	7.7	2.4	4.0	6.0	7.7	2.4	4.0	6.0	7.7
U^E_a [m/s]	1.30	1.24	0.90	0.80	2.06	2.03	1.90	1.68	2.80	2.81	2.77	2.62
ω [rad/s]	14.06	24.71	38.05	47.56	13.88	25.24	38.70	48.15	14.22	25.74	38.62	48.36
f_g^F [Hz]	2.24	3.93	6.06	7.57	2.21	4.02	6.16	7.66	2.26	4.10	6.15	7.70
φ [rad]	-0.61	-0.88	-1.34	-1.74	-0.60	-0.81	-1.35	-1.44	-0.71	-0.75	-0.81	-0.74
R^2	0.97	0.98	0.98	0.97	0.98	0.98	0.98	0.98	0.97	0.98	0.98	0.98

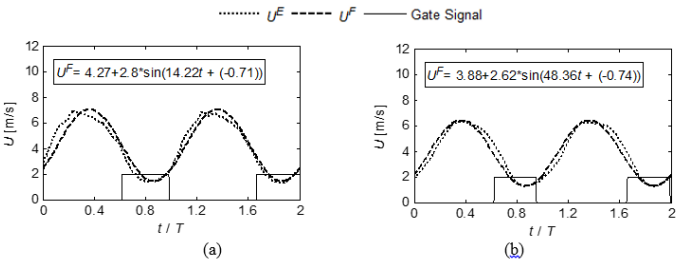

Figure 3. Variation as a function of time, t, of the measured flow in the test section, U^E, and the sinusoidal curve fitted data, U^F, from eqn. (1) at nominal gust frequencies (a) f_g^N = 2.4 Hz, T = 0.41 s, (b) 7.7 Hz, T = 0.129 s, and fan motors speed f_m = 40 Hz (i.e. mean wind speed U^E_{mv} = 4.5 to 5.5 m/s); T is the period of a cycle. Gate signal high indicates the position where the rotating gate closes the wind tunnel duct (minimum speed of the gust).

International Journal Of Scientific & Engineering Research, Volume 7, Issue 6, June-2016
ISSN 2229-5518

As shown in fig. 3 the variation of the measured flow in the test section, U^E, and the sinusoidal curve fitted data, U^F, are presented for f_g^N = 2.4 and 7.7 Hz. A good agreement between the time variation of velocity measurements and the sinusoidal approximation is obtained, and as shown in table 1 the regression coefficient R^2 is close to 1. Therefore, the gust generated by this wind tunnel can be considered to follow a sinusoidal law. As shown in table 1, the gust wind frequency obtained by the sinusoidal fitting data, f_g^F, nearly follows the nominal gust frequency, f_g^N. The amplitude of the sinusoidal oscillations of the curve fitted data, U_a^F, decreases as the gust frequency f_g^N increases (table 1).

3. Theoretical model

In this section a theoretical model is developed based on the mass conservation equation taking in to account of polytropic evolution inside the air reservoir (see Christians [26]), as well as additional considerations, such as the exit conditions and empirical pressure-loss coefficients for the flow through the vent holes. The thermodynamic properties of the gas in the reservoir are considered homogeneous, and no spatial gradients are taken into account (see Holmes [1, 10] for more information). This is an idealization of the evolution because heat transfer from the walls could induce a convective flow. In the homogeneous model no gradients are considered, and the heat transfer with the container walls is modelled in an approximate way by the polytropic coefficient *n*, which in the worst case can be assumed to be close to the isothermal case *n* = 1. In the present experimental setup, the air reservoir is made of wood which is a heat insulator and the room temperature is constant, therefore no significative temperature gradients exists. If there is no influence of heat transfer through the reservoir wall, an adiabatic behaviour takes place and the polytropic coefficient is *n* = □. In the case that some heat transfer takes place, the air temperature will tend to follow the temperature of the container walls and *n* < □, especially in the isothermal limit, when *n* = 1. This case takes place when the flow is slow and there is a temperature gradient between the fluid and the wall. The influence of the wall temperature changes are not considered here, as its variation is small in the time intervals typical of vent phenomena. Air can be considered as a perfect gas in the pressure range involved in the applications of the model. The developed model can also be applied to the case where the room has additional vents whose net size is far smaller than that reference vent.

3.1 *Implementation of the model*

Taking into account the abovementioned assumption of homogeneous distribution of thermodynamic properties, the mass variation in the reservoir is given by,

$$V_R \frac{\mathrm{d}\rho_0}{\mathrm{d}t} = -\rho_0 S U_{vh}\,, \tag{2}$$

where V_R is the reservoir volume, U_{vh} the speed of the air flowing through the hole, ρ_0 the density of the air both in the reservoir and the hole (considering that U_{vh} is small compared to the sound speed), and *S* the section area of the vent hole. The evolution of the thermodynamic properties within the reservoir can be described by a polytropic law (see Christians [26]),

$$\frac{P_0(t)}{\rho_0(t)^n} = \frac{P_r}{\rho_r{}^n}\,, \tag{3}$$

$$\rho_0(t) = \rho_r \left(\frac{P_0(t)}{P_r}\right)^{\frac{1}{n}}\,, \tag{4}$$

and, therefore,

$$\frac{\mathrm{d}\rho_0}{\mathrm{d}t} = \frac{\rho_r}{nP_r}\left(\frac{P_0(t)}{P_r}\right)^{\frac{1}{n}-1}\frac{\mathrm{d}P_0}{\mathrm{d}t}\,, \tag{5}$$

where the subscripts *r* and 0 stands for initial (or reference) and instantaneous stagnation conditions in the reservoir, respectively. Concerning the flow through the vent hole, the case considered is that where the pressure jump is small to achieve small mechanical loads on the walls. Therefore, a low speed jet is formed at the hole and incompressible flow conditions through the hole can be considered, and in fact are assumed in writing eqn. (2) as the air density in the hole is considered the same as ρ_0 (no compressibility effects were included i.e., no changes of density due to speed changes are considered as the Mach number is small).

The pressure jump across the vent hole, ΔP, is a consequence of the pressure loss through the vent hole

$$\Delta P = P_0 - P_e = \frac{1}{2}\rho_0(t) U_{vh}^2 \xi\, \mathrm{sign}(U_{vh}), \tag{6}$$

where ξ is the total pressure loss coefficient and ΔP is measured by pressure transducer TR_1, and $\Delta P_e = P_e - P_r \rightarrow P_e = \Delta P_e + P_r$, where ΔP_e is the pressure difference between wind tunnel pressure, P_e, and barometric pressure P_r. ΔP_e is measured by pressure transducer TR_2 and P_r is obtained from the lab absolute pressure transducer.

From eqn. (6)

$$U_{vh} = \sqrt{\frac{2|\Delta P|}{\rho_0(t)\xi}}\,\mathrm{sign}(\Delta P)\,, \tag{7}$$

and to determine the air density, the internal pressure should be known

$$P_0 = P_e + \Delta P = P_r + (\Delta P + \Delta P_e) \tag{8}$$

Substituting eqn. (7) into eqn. (2) gives

$$\left(\frac{\mathrm{d}\rho_0}{\mathrm{d}t}\right)^2 = \rho_0 \left(\frac{S}{V_R}\right)^2 \frac{2|\Delta P|}{\xi} \tag{9}$$

Taking into account that

$$n\frac{\mathrm{d}\rho_0}{\rho_0} = \frac{\mathrm{d}P_0}{P_0}\,,\ \mathrm{d}\rho_0 = \frac{\rho_0}{n}\frac{\mathrm{d}P_0}{P_0} \tag{10}$$

and substituting eqn. (10) into eqn. (9) one obtains

$$|\Delta P| = \left(\frac{V_R}{S}\right)^2 \frac{\xi}{2n^2}\frac{\rho_0(t)}{P_0(t)^2}\left(\frac{\mathrm{d}P_0}{\mathrm{d}t}\right)^2\,, \tag{11}$$

and from eqn. (7) and (2)

$$\Delta P = -|\Delta P|\,\mathrm{sign}\left(\frac{\mathrm{d}P_0}{\mathrm{d}t}\right). \tag{12}$$

From eqn. (11) it can be deduced that if the pressure jump ΔP is zero then the derivative of the internal pressure inside the air reservoir P_0, with respect to time, *t*, is equal to zero. At this point the pressure jump ΔP changes its sign (then the flow through the vent hole is reversed

International Journal Of Scientific & Engineering Research, Volume 7, Issue 6, June-2016
ISSN 2229-5518

and the derivative of the density should change sign). This behaviour is also apparent in the experimental results.

In the following sections, the experimentally measured and theoretically predicted pressure differences will be distinguished by using the following notation: experimental pressure jump, ΔP^E; experimental external pressure variation, ΔP_e^E ; experimental internal pressure, P_0^E ; and theoretically predicted pressure jump, ΔP^T. The theoretical pressure jump is obtained from eqn. (11) and eqn. (12)

$$\left|\Delta P^T\right| = \left(\frac{V_R}{S}\right)^2 \frac{\xi}{2n^2} \frac{\rho_0(t)}{P_0(t)^2} \left(\frac{\mathrm{d}P_0^E}{\mathrm{d}t}\right)^2 , \tag{13}$$

$$\Delta P^T = -\left|\Delta P^T\right| \mathrm{sign}\left(\frac{\mathrm{d}P_0^E}{\mathrm{d}t}\right), \tag{14}$$

where $P_0^E(t)$ is obtained from eqn. (8) by introducing the experimental pressure jump measurements ΔP^E and experimental external pressure variations ΔP_e^E , which are measured by the pressure transducers TR_1 and TR_2, respectively.

3.2 *Small pressure jumps across the vent holes*

The above derived model (eqn. (14)) is the model proposed to measure the pressure jumps from the venting holes, but this paper is mainly focused in the case where a small pressure jump across the vent holes can appear. To do this, the results obtained from the experiments (pressure jumps) with various vent hole sizes (R_{vh} =0.5 mm to 12.5 mm) need to be filtered with a condition which should be fulfilled to obtain results corresponding to a small pressure jump across the vent holes. Therefore, the problem formulation in eqn. (3) and eqn. (9), are rewritten in dimensionless form by using as reference magnitudes the characteristic time, t_c, density, ρ_r , and reference pressure P_r, and small pressure jump δ ,

$$t = t_c T,\ \rho_0(t) = \rho\rho_r,\ P_0(t) = pP_r,\ P_e = p_e P_r,\ \Delta P = \delta P_r , \tag{15}$$

$$p = \frac{P_0(t)}{P_r},\ \rho = \frac{\rho_0(t)}{\rho_r},\ p_e = \frac{P_e}{P_r},\ \delta = \frac{\Delta P}{P_r},\ t_c = \frac{V_R}{Sa_r}\sqrt{\frac{\xi\gamma}{2}},$$

$$a_r = \sqrt{\frac{\gamma P_r}{\rho_r}} . \tag{16}$$

In the small pressure jump depressurization range, the assumption $\delta << 1$ can help an asymptotic solution to be found. $\delta << 1$ means that $\Delta P << P_r$ which is the most frequent case ($\Delta P < 10^3$ Pa and $P_r \approx 10^5$ Pa).

As a first step, the variables of the problem should be expressed as power series expansion of a small parameter $\nu << 1$, as follows:

$$p = p_e + \nu p_1. \tag{17}$$

Substituting eqn. (16) into eqn. (17) gives

$$\frac{P_0(t)}{P_r} = \frac{P_e}{P_r} + \nu p_1 = \frac{P_e}{P_r} + \delta ,$$

where $\delta = \nu p_1$ is the dimensionless pressure jump (i.e. the pressure load on the reservoir walls) and the density is

$$\rho_0(t) = \rho_r \left(p_e + \delta\right)^{\frac{1}{n}}. \tag{18}$$

Substituting eqn. (18) in eqn. (9) one obtains

$$\left(\frac{\rho_r}{nP_r}\left(\frac{P_e + \Delta P}{P_r}\right)^{\frac{1}{n}-1} \frac{\mathrm{d}(P_e + \Delta P)}{\mathrm{d}t}\right)^2 = \rho_0(t)\left(\frac{S}{V_R}\right)^2 \frac{2|\Delta P|}{\xi} . \tag{19}$$

Let us assume that a sudden wind gust gives rise, g, to a pressure evolution outside the building, which is small compared with the atmospheric pressure, and then the external pressure from eqn. (16) can be written as

$$P_e = P_r(1 + \varepsilon g\ )\ ;\ \Delta P = \delta P_r\ ;\ \frac{P_0(t)}{P_r} = 1 + \varepsilon g + \delta , \tag{20}$$

where $\varepsilon = \frac{P_e^{\max}}{P_r} - 1$, (21)

which determines the gust amplitude, $P_e^{\max}$ is the maximum value of the external pressure, and $g(t)$ is the raised dimensionless gust as a function of time.

From eqn. (5) and (9) one obtains

$$\frac{\rho_r}{nP_r}\left(\frac{P_0(t)}{P_r}\right)^{\frac{1}{n}-1} \frac{\mathrm{d}P_0}{\mathrm{d}t} = -\rho_0^{1/2} \frac{S}{V_R}\sqrt{\frac{2|\Delta P|}{\xi}}\,\mathrm{sign}(\Delta P) \tag{22}$$

Substituting eqn. (20) into eqn. (22) gives

$$\left[\frac{\rho_r}{nP_r}\left(1 + \varepsilon g + \delta\right)^{\frac{1}{n}-1} \frac{P_r \mathrm{d}\left(1 + \varepsilon g + \delta\right)}{\mathrm{d}t}\right]^2 = \rho_r \left(\frac{S}{V_R}\right)^2 \frac{2|\delta|P_r}{\xi} . \tag{23}$$

In the case of large radius, R_{vh}, vent holes the condition $\varepsilon g >> \delta$ holds (due to the small pressure jumps across large diameter holes). Therefore, neglecting small terms, then eqn. (23) leads to

$$\left[\frac{\rho_r}{n}\frac{\mathrm{d}(\varepsilon g)}{\mathrm{d}t}\right]^2 = \rho_r \left(\frac{S}{V_R}\right)^2 \frac{2|\delta|P_r}{\xi} , \tag{24}$$

and thus,

$$|\delta| = \frac{1}{n^2}\left(\frac{V_R}{S}\right)^2 \frac{\gamma\xi\rho_r}{2\gamma P_r}\left[\frac{\mathrm{d}(\varepsilon g)}{\mathrm{d}t}\right]^2 . \tag{25}$$

From the definition (eqn. (16)) of the characteristic vent time, t_c, the first part of the left-hand side can be expressed as follows,

$$t_c^2 = \left(\frac{V_R}{S}\right)^2 \frac{\gamma\xi\rho_r}{2\gamma P_r} = \left(\frac{V_R}{Sa_r}\right)^2 \frac{\xi\gamma}{2} . \tag{26}$$

Rewriting eqn. (25) by using eqn. (26) then gives

$$|\delta| = \frac{t_c^2}{n^2}\left[\frac{\mathrm{d}(\varepsilon g)}{\mathrm{d}t}\right]^2 . \tag{27}$$

If the radius of the vent hole, R_{vh}, is large then both t_c and the pressure jump δ are small (due to the small pressure jumps that arise across large size holes).

International Journal Of Scientific & Engineering Research, Volume 7, Issue 6, June-2016
ISSN 2229-5518

The dimensionless gust pressure $g\left(\frac{t}{t_g}\right)$ is a function of Θ where $\Theta = \frac{t}{t_g}$ and t_g is the characteristic time of the gust evolution. Therefore, $g\left(\frac{t}{t_g}\right) = g(\Theta)$ and eqn. (27) can be written as

$$|\delta| = \frac{t_c^2}{n^2 t_g^2}\left[\frac{\mathrm{d}(\varepsilon g)}{\mathrm{d}\Theta}\right]^2 = \frac{K^2\varepsilon^2}{n^2}\left[\frac{\mathrm{d}(g)}{\mathrm{d}\Theta}\right]^2 , \qquad (28)$$

where $\frac{\mathrm{d}(g)}{\mathrm{d}\Theta} = \mathrm{O}(1)$ and $K = \frac{t_c}{t_g}$ is the ratio of the characteristic vent time to the gust pressure variation time.

From eqn. (28) the order of magnitude of the δ (only in the case $\varepsilon g >> \delta$) can be obtained

$$|\delta| \sim K^2\varepsilon^2 << \varepsilon \rightarrow K^2 << \frac{1}{\varepsilon} \rightarrow K << \frac{1}{\sqrt{\varepsilon}} . \qquad (29)$$

Eqn. (29) is the condition to select the experimental configurations, which gives the appropriate data to analyse the range of small pressure jumps across the vent holes. To analyze the experimental results, the dimensionless amplitude of the external pressure in experiments ε^E is defined from eqn. (21) as follows,

$$\varepsilon^E = \left(\frac{P_e^{\max E} - P_r}{P_r}\right). \qquad (30)$$

Considering the condition of applicability of the model for the experimental results, using eqns. (30) and (29) one obtains

$$K^E << \frac{1}{\sqrt{\varepsilon^E}} , \qquad (31)$$

where superscript *E* represents the values taken from experiments. As a further step, the results obtained from the experimental setup (shown in table 2) have been screened to fulfil condition (31).

Table 2. Experimental setup.

Experimental setup	
Parameters	Values
Reservoirs volume, V_R	0.022 m³, 0.011 m³,0.0062 m³, 0.0033 m³, and 0.0016 m³
Vent hole radius, R_{vh}	0.5 mm, 1.5 mm, 2.5 mm, 5 mm, 7 mm, 9 mm, 10 mm, 11 mm, and 12.5 mm
Nominal gust frequency, f_g^N	2.4 Hz, 4.0 Hz, 6.0 Hz, and 7.7 Hz
Fan rotational speed, f_m	40 Hz (i.e. U^E_{mv} = 5.5 to 6 m/s)
Length of the gate chord, L_{gc}	380 mm

4. Experimental results

As shown in table 3, for the obtained data from experiments, the minimum value of $1/\sqrt{\varepsilon^E}$ by using (30) is close to 11. It also notable that, the influence of the volume and hole diameter is small. The influence of the gust frequency is due to the change in the pressure evolution inside the wind tunnel. From these data, condition (31) can be rewritten as $K^E << 10$.

Table 3. Variation of $1/\sqrt{\varepsilon^E}$ as a function of the nominal gust frequency, f_g^N, vent hole radius, R_{vh}, and volume of the air reservoir, V_R.

R_{vh} [mm]	0.50	1.50	2.50	5.00	7.00	9.00	10.00	11.00	12.50
f_g^N [Hz]									
				V_R = 0.022 m³					
2.4	14.8	14.8	15.2	14.7	14.4	14.8	14.2	14.8	14.5
4.0	13.3	13.2	13.3	13.2	13.2	13.2	13.2	13.1	13.3
6.0	12.0	12.0	12.0	11.8	11.8	11.9	11.9	11.9	11.8
7.7	11.2	11.4	11.4	11.3	11.3	11.3	11.3	11.3	11.3
				V_R =0.011 m³					
2.4	14.9	14.9	14.9	14.9	14.9	15.0	15.0	14.9	15.0
4.0	13.3	13.3	13.3	13.3	13.4	13.4	13.5	13.3	13.3
6.0	12.0	12.0	12.0	12.0	12.0	12.0	12.1	12.0	12.0
7.7	11.4	11.4	11.4	11.4	11.5	11.5	11.5	11.5	11.4
				V_R =0.0062 m³					
2.4	15.4	15.3	15.2	15.0	14.9	14.7	14.7	14.5	14.5
4.0	14.0	13.9	13.8	13.7	13.5	13.4	13.4	13.2	13.3
6.0	12.1	12.1	12.0	12.0	12.0	12.0	12.0	12.0	12.0
7.7	11.4	11.4	11.4	11.4	11.4	11.4	11.4	11.4	11.4
				V_R =0.0033 m³					
2.4	15.1	15.0	15.0	14.9	14.7	14.6	14.6	14.5	14.4
4.0	13.1	13.2	13.2	13.2	13.2	13.2	13.2	13.3	13.2
6.0	11.9	11.9	11.9	11.9	11.9	11.9	11.9	11.9	12.0
7.7	11.5	11.5	11.5	11.5	11.5	11.5	11.5	11.5	11.5
				V_R =0.0016 m³					
2.0	14.9	14.5	14.5	14.5	14.3	13.9	14.5	14.4	14.6
4.0	13.3	13.3	13.3	13.3	13.3	12.6	13.3	13.2	13.2
6.0	12.0	12.0	12.0	12.0	12.0	11.5	12.0	12.0	12.0
7.7	11.4	11.4	11.4	11.3	11.3	11.1	11.3	11.3	11.4

As shown in fig. 4 and table 4, the condition $K^E << 10$ is fulfilled in the cases with a vent hole radius R_{vh} = 9, 10, 11, 12.5 mm, air reservoir volume, V_R = 0.022, 0.011, 0.0062, 0.0033, 0.0016 m³, and nominal gust frequency f_g^N = 2.4, 4.0, 6.0, 7.7 Hz. Therefore, in the present paper the experimental results corresponding to these configurations were selected for the analysis.

The results obtained for the pressure jump estimated by theoretical model ΔP^T from eqn. (14), for measured pressure jump, ΔP^E, and for measured external gust pressure, ΔP_e^E, for the configurations with air reservoir volume, V_R = 0.022 m³ and 0.0033 m³, vent hole radius, R_{vh} = 12.5 mm are shown in the following figures.

Table 4. Variation of K^E as a function of the nominal gust frequency, f_g^N, vent hole radius, R_{vh}, and volume of the air reservoir, V_R.

International Journal Of Scientific & Engineering Research, Volume 7, Issue 6, June-2016
ISSN 2229-5518

R_{vh} [mm]	0.50	1.50	2.50	5.00	7.00	9.00	10.00	11.00	12.50
f_g^N [Hz]									
				$V_R = 0.022$ m^3					
2.4	1013.6	113.9	41.2	10.1	5.3	3.2	2.5	2.1	1.7
4.0	1719.8	189.7	69.1	17.3	8.8	5.3	4.3	3.5	2.8
6.0	2575.1	288.1	103.9	25.9	13.3	8.0	6.5	5.4	4.2
7.7	3312.6	367.7	132.8	33.4	16.9	10.3	8.3	6.9	5.3
				$V_R = 0.011$ m^3					
2.4	517.4	57.5	20.9	5.2	2.6	1.6	1.3	1.1	0.8
4.0	848.6	94.4	34.1	8.5	4.3	2.6	2.1	1.8	1.4
6.0	1286.4	143.4	51.1	12.9	6.6	3.9	3.2	2.7	2.0
7.7	1623.7	180.8	65.3	16.2	8.3	5.0	4.1	3.4	2.6
				$V_R = 0.0062$ m^3					
2.4	295.6	32.2	11.7	3.0	1.5	0.9	0.7	0.6	0.5
4.0	478.3	53.0	19.1	4.8	2.4	1.5	1.2	1.0	0.8
6.0	722.0	80.6	29.1	7.2	3.7	2.2	1.8	1.5	1.2
7.7	910.4	101.3	36.7	9.1	4.7	2.8	2.3	1.9	1.5
				$V_R = 0.0033$ m^3					
2.4	153.4	17.3	6.2	1.5	0.8	0.5	0.4	0.3	0.3
4.0	255.7	28.5	10.1	2.6	1.3	0.8	0.6	0.5	0.4
6.0	386.9	42.7	15.3	3.9	2.0	1.2	1.0	0.8	0.6
7.7	488.8	54.1	19.5	4.9	2.5	1.5	1.2	1.0	0.8
				$V_R = 0.0016$ m^3					
2.4	76.0	8.4	3.0	0.8	0.4	0.2	0.2	0.2	0.1
4.0	122.8	13.7	5.0	1.2	0.6	0.4	0.3	0.3	0.2
6.0	187.9	20.8	7.6	1.9	1.0	0.6	0.5	0.4	0.3
7.7	238.7	26.5	9.6	2.4	1.2	0.7	0.6	0.5	0.4

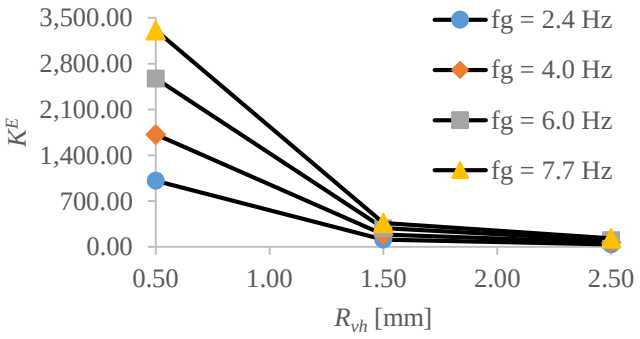

(a1)

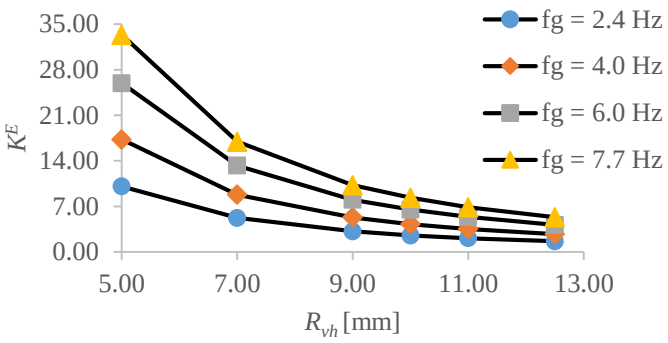

(a2)

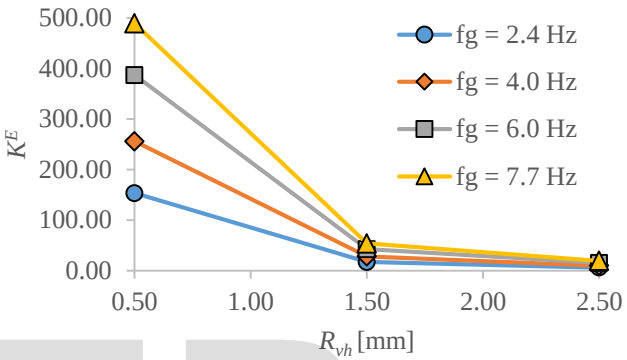

(b1)

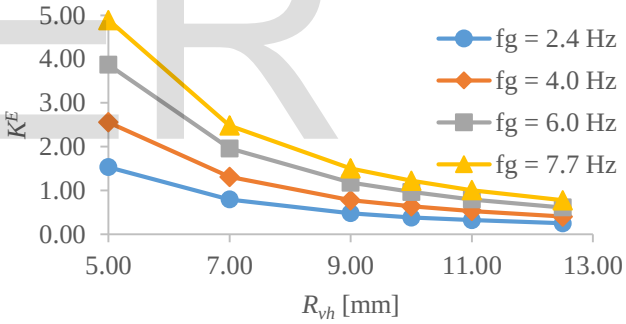

(b2)

Figure 4. Variation of the characteristic vent time, K^E, as a function of radius of the vent holes, R_{vh}, nominal gust frequency fg, and volume of the air reservoir, (fig. a1 & a2) $V_R = 0.022$ m^3, (fig. b1&b2 $V_R = 0.0033$ m^3, fan speed, $f_m = 40$ Hz (i.e. mean flow speed $U_{mv} = 5.5$ to 6 m/s).

As shown in fig. 5, the pressure jump predicted by the theoretical model, ΔP^T (eqn. (14)) and measured pressure jump, ΔP^E, are not in agreement, which is hypothesized to be caused by the assumed value of the pressure loss coefficient, $\xi = 1$. In a steady flow case, the assumed value of $\xi = 1$ or 1.5 for smooth and rough surfaced vent holes, respectively [24]. However, in our case, as the flow is unsteady, the value of ξ is unknown. So that it will be considered as a parameter to be determined by fitting the results of the model to the experimental results as described in the following paragraph.

International Journal Of Scientific & Engineering Research, Volume 7, Issue 6, June-2016
ISSN 2229-5518

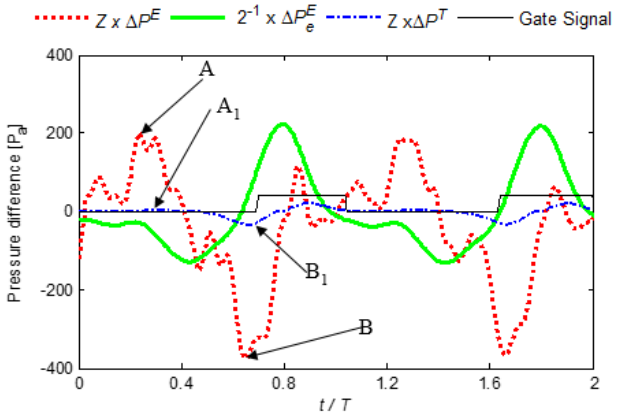

Figure 5. Variation of the measured pressure jump, ΔP^E, theoretical pressure jump, ΔP^T, and wind tunnel gust pressure, $\Delta P_e{}^E$ as a function of time, t, measured in the experimental setup with f_m = 40 Hz (i.e. U^E_{mv} = 5 to 6 m/s), nominal gust frequency, f_g^N = 7.7 Hz, T = 0.129 s. Gate signal high indicates the position where the rotating gate closes the wind tunnel duct (minimum speed of the gust), and R_{vh} = 12.5 mm. V_R = 0.0033 m^3, Z = 10; T is the period of a cycle; pressure loss coefficient ξ =1; Z is a scale factor variable.

4.1 *Empirical estimation of the pressure loss coefficient*

The measured pressure jump ΔP^E (See fig. 5) has positive and negative peak values with different scale factors, which suggests that the pressure loss coefficient is different for positive and negative jumps. Therefore, a constant value of the pressure loss coefficient ξ is not able to fit both pressure jump directions. As a solution to this problem, different pressure loss coefficients for positive and negative side pressure jumps are considered. The method to determine them is by fitting the maximum and minimum peak values of the theoretical and measured pressure jumps $\Delta P^T_{\max}$ and $\Delta P^E_{\max}$, $\Delta P^T_{\min}$ and $\Delta P^E_{\min}$ respectively , by using the following empirical relationships,

$$\xi_{max} = \frac{\Delta P^E_{max}}{\Delta P^T_{max}} \text{ and } \xi_{min} = \frac{\Delta P^E_{min}}{\Delta P^T_{min}}, \qquad (32)$$

where $\xi_{\max}$ and $\xi_{\min}$ are fitting parameters than can be considered as the pressure loss coefficients for positive and negative pressure jumps, respectively.

The positive maximum values (see fig. 5) of the measured and theoretical signals, A and A_1, respectively, correspond to positive peaks that cannot be correlated to each other. Therefore, the theoretical positive peak A_1, which is closer to the experimental peak A, has been chosen and used to find the value of ξ_{max}. In this way, the maximum values (for positive jumps) are matched. In the case of negative peaks, measured and theoretical values are B and B_1 respectively, and both peaks are clearly identified and correlated.

The results of experimental and theoretical pressure jumps, ΔP^E and ΔP^T, respectively, and external gust pressure ΔP_e^E are presented in the figs. 6 and 7 (ΔP^T, has been calculated using the values obtained in each phase of ξ_{max} and ξ_{min}.).

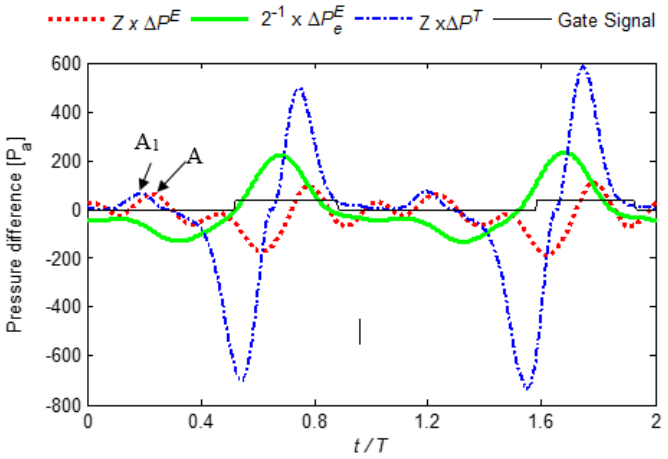

(a)

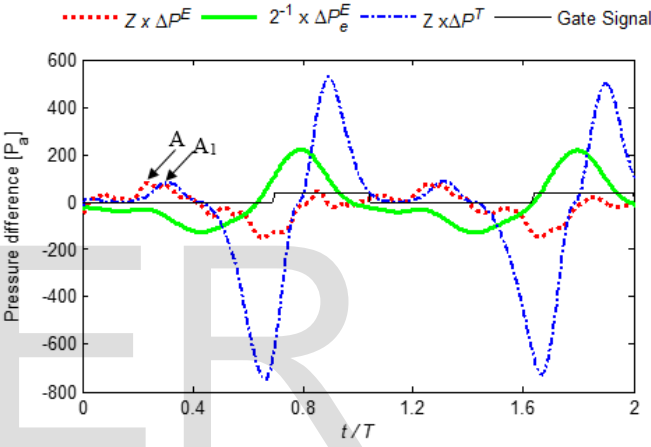

(b)

Figure 6. Same as fig.5, but fitting the positive side pressure jumps with a positive pressure loss coefficient, $\xi = \xi_{\max}$ (a) reservoir volume V_R = 0.022 m^3, Z = 1, and (b) reservoir volume V_R = 0.0033 m^3, Z = 4.

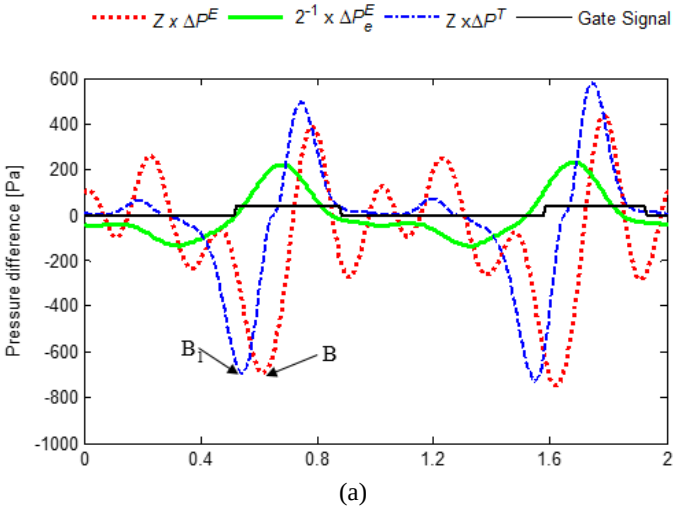

(a)

International Journal Of Scientific & Engineering Research, Volume 7, Issue 6, June-2016
ISSN 2229-5518

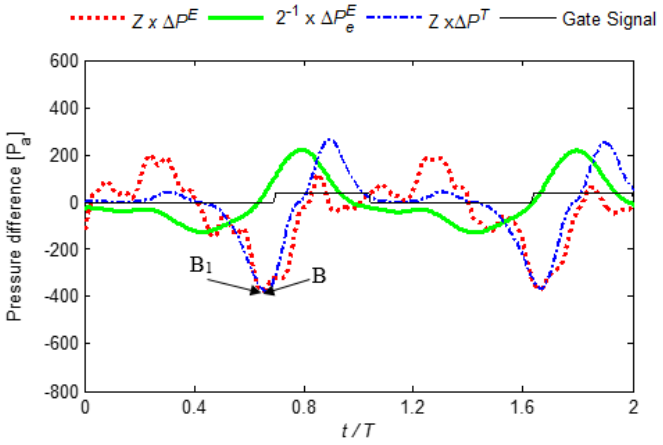

(b)

Figure 7. Same as fig. 5, but fitting the negative side pressure jumps with a negative pressure loss coefficient, $\xi = \xi_{\min}$ (a) V_R = 0.022 m^3, Z = 4, and (b) V_R = 0.0033 m^3, Z = 10.

As shown in figs. 6 and 7, concerning the shape of the curves close to the peaks, in both (positive and negative pressure jumps) cases a good agreement is obtained between measured and theoretical results, although a small phase delay is apparent. Further study would be needed to analyse this phase delay between the theoretical and experimentally measured positive and negative pressure jumps.
As shown in the tables 5, 6 and fig. 8, (the definition for the flow coefficient, α, can be found in section 4.2) the value of the positive and negative pressure loss coefficients, ξ_{max}, and ξ_{min}, increases and decreases, respectively, as the gust frequency increases which is a curious outcome from these experiments.

4.2 *Relationship between the flow coefficient, α and pressure loss coefficient, ξ*
The mass flow rate through a vent hole, in steady flow conditions is given by

$$Q_m = \rho_0(t) S U_{vh} = \alpha S \sqrt{2\rho_0(t)\Delta P}\,, \qquad (33)$$

where α is the flow coefficient (denoted with the letter K in White [24]).
Substituting eqn. (6) into eqn. (33) the following relationship is obtained

$$\rho_0(t)^2 S^2 U_{vh}^2 = \alpha^2 S^2 \rho_0(t)^2 U_{vh}^2 \xi\,, \qquad (34)$$

and therefore α and ξ are related through

$$\alpha^2 = \frac{1}{\xi} \rightarrow \alpha = \frac{1}{\sqrt{\xi}}\,. \qquad (35)$$

From the empirical estimation of the pressure loss coefficients, ξ_{max}, and ξ_{min}, the respective flow coefficients can also be defined from eqn. (33) as

$$\alpha_{\max} = \frac{1}{\sqrt{\xi_{\max}}} \quad \text{and} \quad \alpha_{\min} = \frac{1}{\sqrt{\xi_{\min}}}\,. \qquad (36)$$

Table 5. Positive pressure jumps. Values of the total pressure loss coefficient, ξ_{max}, and flow coefficient, α_{max}, as a function of the nominal gust frequency, f_g^N, and vent hole radius R_{vh} = 9, 11, 12.5 mm; reservoir volume V_R = 0.022 m^3, 0.011 m^3, 0.0062 m^3, 0.0033 m^3, and 0.0016 m^3.

R_{vh} [mm]	9.00		11.00		12.50	
f_g^N [Hz]	ξ_{max}	α_{max}	ξ_{max}	α_{max}	ξ_{max}	α_{max}
			V_R = 0.022 m^3			
2.4	0.5	1.36	4.8	0.46	11.4	0.30
4.0	1.2	0.90	4.6	0.47	12.0	0.29
6.0	1.4	0.84	6.4	0.40	14.3	0.26
7.7	1.6	0.78	7.3	0.37	15.2	0.26
			V_R = 0.011 m^3			
2.4	6.8	0.38	27.0	0.19	33.8	0.17
4.0	7.0	0.38	28.2	0.19	55.9	0.13
6.0	7.7	0.36	29.7	0.18	58.9	0.13
7.7	11.5	0.29	35.7	0.17	66.4	0.12
			V_R = 0.0062 m^3			
2.4	37.6	0.16	113.9	0.09	153.0	0.08
4.0	27.0	0.19	117.8	0.09	154.9	0.08
6.0	32.5	0.18	120.6	0.09	156.7	0.08
7.7	38.2	0.16	129.6	0.09	215.9	0.07
			V_R = 0.0033 m^3			
2.4	6.2	0.40	138.4	0.08	252.8	0.06
4.0	16.4	0.25	141.2	0.08	258.8	0.06
6.0	22.2	0.21	146.5	0.08	270.7	0.06
7.7	25.5	0.20	202.6	0.07	282.3	0.06
			V_R = 0.0016 m^3			
2.4	6.7	0.39	13.8	0.27	5.6	0.42
4.0	28.9	0.19	75.5	0.12	74.0	0.12
6.0	39.7	0.16	86.0	0.11	80.7	0.11
7.7	74.9	0.12	122.0	0.09	96.9	0.10

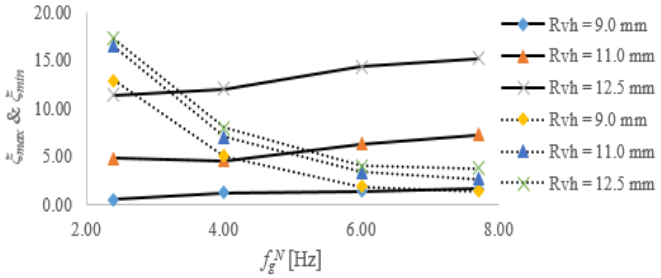

(a)

International Journal Of Scientific & Engineering Research, Volume 7, Issue 6, June-2016
ISSN 2229-5518

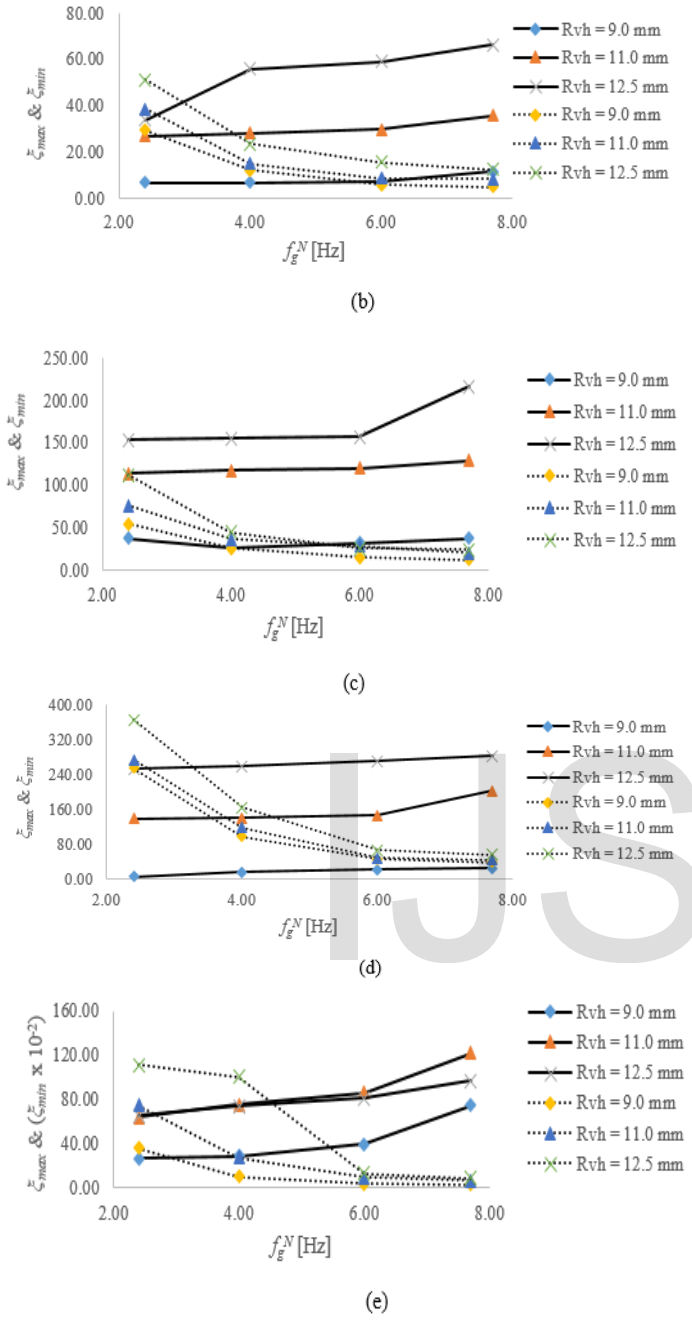

Figure 8. Variation of the total pressure loss coefficients, ξ_{max} and ξ_{min}, referenced to positive (solid lines) and negative (dotted lines) pressure jumps, respectively, as a function of the nominal gust frequency, f_g^N, and radius of the vent hole, R_{vh} = 9, 11, 12.50 mm; reservoir volume V_R = (a) 0.022 m^3, (b) 0.011 m^3, (c) 0.0062 m^3, (d) 0.0033 m^3, and (e) 0.0016 m^3.

Table 6: Negative pressure jumps. Values of the total pressure loss coefficient, ξ_{min}, and flow coefficient, α_{min}, as a function of the nominal gust frequency, f_g^N, and vent hole radius R_{vh} = 9, 11, 12.5 mm; reservoir volume V_R = 0.022 m^3, 0.011 m^3, 0.0062 m^3, 0.0033 m^3, and 0.0016 m^3

R_{vh} [mm]	9.00		11.00		12.50	
f_g^N [Hz]	ξ_{min}	α_{min}	ξ_{min}	α_{min}	ξ_{min}	α_{min}
			V_R = 0.022 m^3			
2.4	12.9	0.24	16.5	0.24	17.2	0.24
4.0	5.0	0.35	7.1	0.35	8.0	0.35
6.0	1.9	0.50	3.4	0.50	4.1	0.50
7.7	1.4	0.51	2.7	0.51	3.8	0.51
			V_R = 0.011 m^3			
2.4	29.4	0.24	38.6	0.24	51.2	0.14
4.0	12.3	0.35	15.1	0.35	23.4	0.21
6.0	6.1	0.50	8.7	0.50	15.8	0.25
7.7	5.0	0.51	8.6	0.51	12.4	0.28
			V_R = 0.0062 m^3			
2.4	54.7	0.24	76.0	0.24	112.4	0.09
4.0	25.8	0.35	36.8	0.35	45.2	0.15
6.0	15.4	0.50	28.5	0.50	26.1	0.20
7.7	13.1	0.51	20.3	0.51	24.7	0.20
			V_R = 0.0033 m^3			
2.4	254.4	0.24	273.9	0.24	365.5	0.05
4.0	97.4	0.35	118.2	0.35	163.9	0.08
6.0	46.5	0.50	49.7	0.50	66.1	0.12
7.7	38.2	0.51	44.0	0.51	56.7	0.13
			V_R = 0.0016 m^3			
2.4	3559	0.24	7483	0.24	11131	0.01
4.0	1014	0.35	2723	0.35	10032	0.01
6.0	376	0.50	950	0.50	1319	0.03
7.7	287	0.51	639	0.51	907	0.03

Concerning the results of the flow coefficient, the reference data can be found in fig. 6.41 of White [24]. (In that book, the flow coefficient is denoted with the letter K, but in the current work the letter K is assigned to the value of a constant which relates ε and $|\delta|$ (eqn. (29)). To avoid confusion the flow coefficient in the present work, it has been renamed with the Greek letter α.) The relationship between the flow coefficient α and pressure loss coefficient ξ (eqn. (36)) allows the relevant results obtained here to be compared with the existing data [24]. As a result of the comparison the following points are outlined.

International Journal Of Scientific & Engineering Research, Volume 7, Issue 6, June-2016
ISSN 2229-5518

The flow coefficient given in the literature α (White [24]) is obtained under steady flow conditions and refers to a fluid flowing from a tube to another tube with larger diameter. α is a function of the ratio of the diameters $\beta = d/D$, where D is the diameter of the larger tube. However, in this paper, the positive pressure jump corresponds to the flow discharge in a cross flow, and the negative pressure jump is the discharge inside a reservoir with fluid at rest, and in both cases the flow can be considered as unsteady. These are the main differences between the experimental conditions of reference for published results and the configurations of the present work.

For the sake of comparison, in both cases the flow is from a hole duct (d = 25 mm) to a much larger room (D = 390 mm), therefore, in both cases the value of β is considered to be less than 0.2 which corresponds to a value of the coefficient α = 0.58 (White [24] chapter 6, fig. 6.41).

As shown in tables 5 and 6, the extreme values obtained for the flow coefficient are α_{max} = 0.90 and 0.10 (except the case with f_g^N = 2.2 Hz, V_R = 0.022 m^3 and D_{vh} = 18 mm) respectively, and for α_{min} are 0.84 and 0.01.

The results obtained in the experiments for positive pressure jumps α_{max} is of the same order of magnitude as the flow coefficient of reference (i.e. α = 0.60). For negative pressure jumps, α_{min} are also in the same range, although the minimum value drops an order of magnitude to 0.01, in the case of small volumes of the reservoirs (i.e. V_R = 0.0016 m^3).

5. Conclusions

The effect of the vent hole diameter on the internal load produced by gusty winds on nonstructural elements (window panels, doors, etc.) has been studied, and considering an experimental configuration similar to the real situation, tangential unsteady flow, experimental data on pressure jumps across vent holes of several diameters D_{vh}, reservoir volumes V_R, with nominal gust frequency f_g^N, fan speed f_m = 40 Hz (equivalent to mean wind speed of U_{mv} = 4.5 to 5.5 m/s) have been obtained. Furthermore, a nonlinear theoretical model based on the gas evolution polytropic law and mass conservation equations has been developed.

From this model a validation condition $K << 1/\sqrt{\varepsilon}$ has been obtained and applied to filter the experimental results for configurations with small pressure jumps across the vent holes which are the most interesting cases. From the results of the selected cases, it has been concluded that the total pressure loss coefficient ξ is not a constant for all the experimental cases, but it is a function of the nominal gust frequency, f_g^N, and the sign of the pressure jump.

Therefore, two total pressure loss coefficients, for the positive and negative pressure jumps, ξ_{max} and ξ_{min}, respectively, have been identified. The values of ξ_{max} and ξ_{min} have been obtained by fitting the maximum and minimum values of the theoretical and measured pressure jumps. This difference may be related to the type of flow associated to each case: a jet discharge in a cross flow for positive pressure jumps, and a discharge inside a reservoir filled with fluid at rest for negative pressure jumps. Further study would be needed to analyse and explain the phase delay between the results of the theoretical and measured negative pressure jumps.

Concerning the results for the flow coefficient α, a relationship between α and the pressure loss coefficient ξ has been obtained and a comparison with the relevant results from the existing literature shows some agreement, in some cases. In any case, a good agreement was not expected, due to the difference in flow conditions.

Finally, it has been shown that the estimation of the pressure jump across the vent hole in an unsteady flow involves a non-linear mathematical model and a non-linear solution. The models developed in previous studies are linear, which might not be suitable to estimate the pressure jumps in unsteady flow cases.

The non-linear model proposed in this paper, taking into account the different values for the positive and negative pressure loss coefficients ξ_{max} and ξ_{min} are able to predict results which are in good agreement with the measured pressure jumps ΔP^E.

Nomenclature

a_r Speed of sound under the reservoir initial conditions
f_g^N Nominal gust frequencies
f_g^F Gust wind frequency obtained by the sinusoidal fitting data
g Sudden rise in wind gust
K Ratio of the characteristic vent time to the gust pressure variation time
L_{gc} Rotating gates with blockage length
Pt_1, Pt_2 and Pt_3 Pressure taps
P_0 Internal pressures of the reservoir
P_e Wind tunnel pressure
P_e^{max} Maximum value of the external pressure
P_r Atmospheric pressure
P_0^E Experimentally measured internal pressure,
R^2 Regression coefficient
R_{vh} Vent hole radius
S Section area of the vent hole
t_c Characteristic vent time
t_g Characteristic time of the gust evolution
U_{mv} Mean speed of gusty winds
U^E Velocity of the flow in the test section
U_a^E Amplitude of the sinusoidal signal
U_{mv}^E Mean value of measured flow
U^F Curve fitted data to the sinusoidal signal
V_R Volume of the reservoir
α Flow coefficient
γ Specific heat ratio
ξ Pressure loss coefficient
ξ_{max} Pressure loss coefficients for positive pressure jump
ξ_{min} Pressure loss coefficients for negative pressure jump
ε Amplitude of the suddenly raised wind gust
ω Angular frequency of the sinusoidal signal
φ The phase referenced to wind blockage gate closing position
ρ_0 Density of the air (inside the reservoir)
ν Small parameter
ΔP Pressure jump across the vent hole
ΔP_e Pressure increment inside the wind tunnel
ΔP^T Theoretically predicted pressure jump
ΔP^E Experimentally measured pressure jump

International Journal Of Scientific & Engineering Research, Volume 7, Issue 6, June-2016
ISSN 2229-5518

ΔP_e^E Experimentally measured external pressure variation

Superscripts

E Values taken from the experiments

N Nominal

Subscripts

R Initial (or reference) conditions in the reservoir

0 Instantaneous stagnation conditions in the reservoir

max Maximum value

min Minimum value

g Gust

References

[1]. Holmes, J.D., 1979. Mean and fluctuating internal pressures induced by wind. In: Proceedings of the Fifth International Conference on Wind Engineering. July, Fort Collins, Colorado, USA, pp. 435–440.

[2]. Euteneuer, G.A., 1971. Einfluss des Windeinfalls auf Innendruck und Zugluft erscheinung in teilweise offenen Bauwerken (Influence of wind flow on internal pressure and creation of drafts in partially open buildings). Der Bauingenieur 46, pp. 355–360.

[3]. Liu, P.H., Saathoff, I., 1981. Building internal pressure: sudden change, Journal of the Engineering Mechanics Division, ASCE 107, pp. 309–321.

[4]. Sharma, R.N., Richards, P.J., 1997. The effect of roof flexibility on internal pressure fluctuations. Journal of Wind Engineering and Industrial Aerodynamics 72, pp. 175–186.

[5]. Vickery, B.J., 1994. Internal pressures and interactions with the building envelope. Journal of Wind Engineering and Industrial Aerodynamics 53, pp. 125–144.

[6]. Liu, H., Rhee, K.H., 1986. Helmholtz oscillation in building models. Journal of Wind Engineering and Industrial Aerodynamics 25, pp. 95–115.

[7]. Vickery, B.J., Bloxham, C., 1992. Internal pressure dynamics with a dominant opening. Journal of Wind Engineering and Industrial Aerodynamics 41, pp. 193–204.

[8]. Ginger, J.D., Mehta, K.C., Yeatts, B.B., 1997. Internal pressures in a low-rise full scale building. Journal of Wind Engineering and Industrial Aerodynamics 72, pp. 163–174.

[9]. Sharma, R.N., Richards, P.J., 2003. The influence of Helmholtz resonance on internal pressure in a low-rise building. Journal of Wind Engineering and Industrial Aerodynamics 91, pp. 807–828.

[10]. Holmes, J.D., 2009. Discussion of net pressures on the roof of a low-rise building with wall openings by Sharma, R.N., Richards, P.J. Journal of Wind Engineering and Industrial Aerodynamics 97, pp. 320–321.

[11]. Kopp, G.A., Oh, J.H., Inculet, D.R., 2008. Wind-induced internal pressures in houses. Journal of Structural Engineering ASCE 134, pp. 1129–1138.

[12]. Sharma, R.N., Richards, P.J., 1997. Computational modelling in the prediction of building internal pressure gain functions. Journal of Wind Engineering and Industrial Aerodynamics 67–68, pp. 815–825.

[13]. Sharma, R.N., 2008. Internal and net envelope pressures in a building having quasi-static flexibility and a dominant opening. Journal of Wind Engineering and Industrial Aerodynamics 96, pp. 1074–1083.

[14]. Harris, R.I., 1990. The propagation of internal pressures in buildings. Journal of Wind Engineering and Industrial Aerodynamics 34, pp. 169–184.

[15]. Holmes, J.D., 2001. Wind Loading of Structures, Spon Press Publications, London, pp. 68–138.

[16]. Chaplin, G., 1997. Turbulent wind interactions with ventilated structures, Ph.D. Thesis, University of Nottingham, United Kingdom.

[17]. Chaplin, G.C., Randall, J.R., Baker, C.J., 2000. The turbulent ventilation of a single opening enclosure. Journal of Wind Engineering and Industrial Aerodynamics 85, pp. 145–161.

[18]. Vickery, B.J., 1986. Gust factors for internal pressures in low rise buildings, Journal of Wind Engineering and Industrial Aerodynamics 23, pp. 259–271.

[19]. NASA SP-8060, 1970. NASA Space Vehicle Design Criteria Compartment Vent, National Aeronautics and Space Administration.

[20]. Sanz-Andres, A., Santiago-Prowald, J., Ayuso-Barea, A., 1997. Spacecraft launch depressurization loads. Journal of Spacecraft and Rockets 34(6), pp. 805–810.

[21]. Ronald, C. D., Walter, G., 2011. Depressurization solutions of vented enclosures during launch. CEAS Space Journal 10.1007/s12567–011–0022–x.

[22]. Sanz-Andres, A. Navarro-Medina, F., 2010. The initiation of rotational motion of a lying object caused by wind gusts. Journal of Wind Engineering and Industrial Aerodynamics 98, pp. 772–783.

[23]. Chevula Sreenadh, 2015. "Aerodynamic loads acting on bluff bodies under wind gusts", Ph.D. thesis, UPM, Madrid. http://oa.upm.es/35504/.

[24]. White, M.F., 2011. Fluid Mechanics, 7th edition, Chapter 6, 7 and 8, McGraw-Hill, New York, NY.

[25]. Chevula, S., Sanz-Andres, A., and Franchini, S., 2015. Aerodynamic external pressure loads on a semi-circular bluff body under wind gusts, Journal of Fluids and Structures. 54, pp. 947–957.

[26]. Christians, J., 2012 Approach for Teaching Polytropic Processes Based on the Energy Transfer Ratio, International Journal of Mechanical Engineering Education, Volume 40, Manchester University Press, UK.

Conflict of Interests

There are no conflict of interests regarding the publication of this paper.